Multipole vibrations of small alkali-metal spheres in a semiclassical description

M. Brack*
Niels Bohr Institute, Blegdamsvej 17, DK-2100 Copenhagen, Denmark
(Received 29 September 1988)

We use the jellium model and a semiclassical version of the energy-density variational method to investigate static properties of spherical metal clusters and obtain excellent agreement with the (averaged) microscopical results. Exploiting random-phase-approximation (RPA) sum-rule techniques, we calculate the eigenmode spectrum for collective multipole vibrations of the electrons, including coupling between surface and volume plasmons. In the classical limit the old Mie result is recovered for the surface plasmons of all multipolarities. From the sum rules, we estimate the static dipole polarizabilities and the position and width of the electric dipole resonance. We find that the RPA estimate of the width is in qualitative agreement with recent experiments on small Na clusters.

I. INTRODUCTION

It is by now well established[1–6] that the jellium model is able to give a fair description of the static properties of clusters of light metals such as Na, K, etc. The density-functional formalism in the Kohn-Sham version combined with the local-density approximation (LDA) has been used by several authors[2–5] to perform self-consistent microscopical calculations of the binding energies, ionization potentials, and dipole polarizabilities of small metal clusters. For the study of collective excitations of the valence electrons in these clusters, linear-response theory in LDA has been applied to calculate the dynamic polarizability.[6] Such self-consistent microscopical calculations become quite time consuming when the size of the clusters increases. It might therefore be of interest to develop a fast numerical approximation which allows one to extend such studies to very large clusters but still ensures self-consistency.

In the present paper, we propose a semiclassical version of the density-functional approach, making use of the extended Thomas-Fermi (ETF) approximation to the kinetic-energy density,[7,8] which has proven to be very successful in reproducing the average static properties of nuclei[9] obtained microscopically by Hartree-Fock (HF) calculations. The TF or ETF kinetic-energy functional has already been used in density-variational calculations to study the average static properties of jellium spheres.[10–12] We shall improve these results by taking the fourth-order gradient corrections[7,8] to the kinetic energy seriously and at the same time using a more flexible trial function[9] for the electron density. Based on the variational electronic ground-state densities thus obtained for jellium spheres, we propose a semiclassical extension of the random-phase-approximation (RPA) sum-rule approach[13] to calculate estimates of the peak positions and widths of collective multipole excitations of the electrons, including coupling of surface and volume plasmons, and to extract the static polarizabilities. We shall show that this method yields similar results as the microscopic time-dependent local-density approximation (TDLDA) linear-response calculations[6] and is at the same time so fast that systematic investigations also of very large clusters (containing thousands of atoms) become possible at very short computing times.

II. GROUND-STATE PROPERTIES

The total energy of a neutral cluster is written[3] as a functional of the local density $\rho(\mathbf{r})$ of the valence electrons:

$$E[\rho]=\int\left[\tau[\rho(\mathbf{r})]+\mathcal{E}_{\rm xc}[\rho(\mathbf{r})]+\tfrac{1}{2}e^2\rho(\mathbf{r})\left[\int\frac{\rho(\mathbf{r}')}{|\mathbf{r}-\mathbf{r}'|}d^3r'\right]+V_I(\mathbf{r})\rho(\mathbf{r})\right]d^3r+E_I\ . \tag{1}$$

Here $\tau[\rho]$ and $\mathcal{E}_{\rm xc}[\rho]$ are the kinetic and the exchange plus correlation energy densities, respectively, the second term is the Hartree Coulomb energy of the electrons, and V_I and E_I are the potential and the total electrostatic energy, respectively, of the ionic background, evaluated as usual in terms of a square density (jellium) of the positive ions and characterized by the Wigner-Seitz radius r_s [or the bulk density $\rho_0^I=3/(4\pi r_s^3)$] and the number Z of atoms. The density $\rho(\mathbf{r})$ is normalized to the number N of valence electrons:

$$\int\rho(\mathbf{r})d^3r=N\ . \tag{2}$$

Instead of varying single-particle wave functions and thus solving the Kohn-Sham equations as done in Refs. 3–5, we perform a restricted variation of the density ρ, utilizing explicitly the semiclassical gradient-expanded functional $\tau[\rho]$ of the extended Thomas-Fermi model including all terms up to fourth order[7,8] *without manipulating their coefficients.* This functional has been shown[8,9] to reproduce very exactly the average—or semiclassical—part of the kinetic energy of a system of fermions in various types of local potentials, in particular, also in nuclei whose densities resemble very much those of the electrons in the jellium model. For $\mathcal{E}_{\rm xc}[\rho]$ we use the LDA functional of Gunnarsson and Lundqvist.[14] We shall presently only apply the method to spherical clusters; the

extension to deformed systems is straightforward.[9]

Our spherical densities $\rho(r)$ are parametrized by the following trial function:

$$\rho(r)=\rho_0\left[1+\exp\left[\frac{r-R}{\alpha}\right]\right]^{-\gamma}. \quad (3)$$

The total energy (1) for a cluster with given atomic number Z is then minimized with respect to the parameters ρ_0, R, α, and γ under the constraint (2). Our approach thus goes beyond similar earlier calculations[10,11] in two respects: we (i) include the fourth-order gradient terms in $\tau[\rho]$ and (ii) have a more flexible density parametrization. In Refs. 10 and 11 the fourth-order terms were omitted; the trial functions used by Snider and Sorbello[11] are the ones we obtain from Eq. (3) with $\gamma=1$ [except for very small clusters; the fact that the slope of the density (3) at $r=0$ is mathematically not zero has no numerical significance for clusters with N larger than four or five]. The relevance of the fourth-order terms in $\tau[\rho]$ and of the variational parameter γ in Eq. (3), which regulates the asymmetry (for $\gamma\neq1$) of the density surface profile around its inflection point, will become evident in the results below. (Typical values of γ are $\simeq0.5$–0.6 for all Na clusters.)

By this restricted semiclassical variational procedure we find densities, potentials, and energies which, of course, exhibit no shell effects, but reproduce very closely the averaged results of the microscopic Kohn-Sham calculations of Refs. 3–5. As a typical example we show in Fig. 1 the variational densities of a neutral Na_{198} cluster alongside the self-consistent effective (Kohn-Sham) potentials. The microscopic results are taken from Ekardt[3] and shown by the solid lines. The dashed lines give our semiclassical results obtained by using the full functional $\tau[\rho]$ up to the fourth-order gradient terms, and the dashed-dotted lines correspond to including only the second-order (i.e., the Weizäcker) gradient correction. Clearly, the fourth-order terms have an important role in bringing our results closer to the microscopical ones. Note that especially the density tail and the "wine-bottle shape" of the potential are perfectly well reproduced. The reason for this wine-bottle shape (the slow increase of the depth of the potential with increasing r) is due to the fact that for a finite cluster the bulk electron density ρ_0 is slightly higher than that of the jellium density (i.e., ρ_0^I), as a result of the surface tension which tends to compress the electrons. A detailed discussion of this mechanism, along with a systematical analysis of our static results, will be found in a forthcoming publication.[15]

In Fig. 2 we show (a) the total energies per electron E/N of neutral ($N=Z$) Na clusters, (b) the ionization potentials $\Phi=E(N=Z-1)-E(N=Z)$, and (c) the electrostatic parts Φ^{es} of the latter, all as functions of the cluster radius $R_I=r_sZ^{1/3}$. The solid lines give our present results and the dots show the results of Ekardt.[3] Clearly we miss the shell effects which are important for the energies shown here. They can be recovered perturbatively either by a Strutinsky procedure[16] or by adding one or two iterations of the Kohn-Sham equation starting from our variational effective potential; corresponding studies are in progress. Note, however, that the semiclassical results nicely represent the averaged microscopical energies. Especially for the electrostatic parts of the ionization potentials, which exhibit almost no shell effects, the agreement is surprisingly good even for $N=4$ ($R_I=6.3a_0$). The fact that the semiclassical binding en-

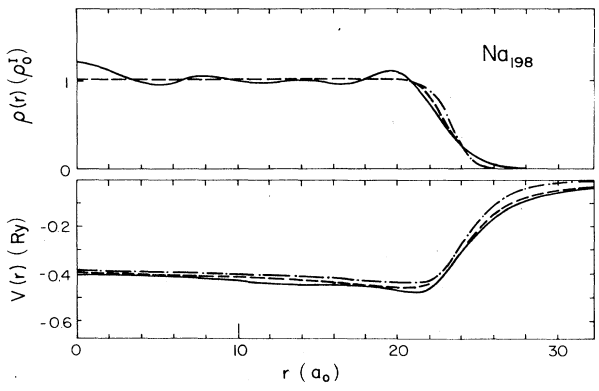

FIG. 1. Variational densities $\rho(r)$ (in units of the jellium bulk density ρ_0^I) and self-consistent effective potentials $V(r)$ (in Rydberg units) for the neutral Na_{198} cluster ($r_s=4$). Solid lines are the results of Ekardt (Ref. 3), dashed and dashed-dotted lines are the present results (see text for details). The parameters in the density Eq. (3) for this cluster are $R=22.516\,25a_0$, $\rho_0=0.003\,765\,31a_0^{-3}$, $\alpha=0.506\,91a_0$, and $\gamma=0.519\,86$; a_0 is the Bohr radius.

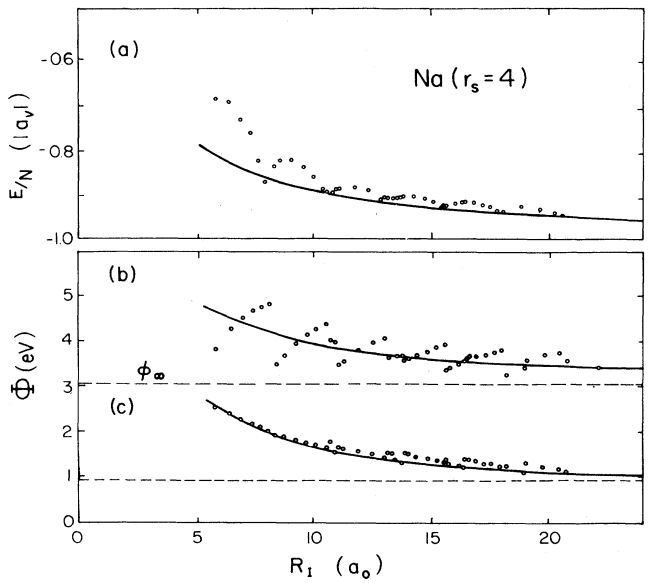

FIG. 2. Upper part (a): total energy per electron (in units of the absolute bulk value $|a_v|$) vs cluster radius R_I for neutral Na clusters. Lower part: Ionization potentials (in eV) of Na clusters vs radius; (b) total Φ, and (c) electrostatic part Φ^{es} (surface barrier). Solid lines are the present results, small circles are the results of Ekardt (Ref. 3).

ergies go almost exactly through the quantum-mechanical energies of those clusters which correspond to the closed-shell configurations is gratifying in that those clusters are spherical and the most stable ones (and easiest to observe experimentally[1]). For the regions in between, the quantum-mechanical energies will be lowered when allowing the clusters to be deformed (see also Ref. 17), which is a mechanism dictated by shell effects, whereas their average energies will slightly increase (the semiclassical energy *is always minimal* for spherical shapes), so that we can expect the agreement to improve considerably in calculations including deformation effects. The situation that the semiclassical energies reproduce best the quantum-mechanical ones in closed-shell configurations has also been observed in density-variational calculations of atomic binding energies[18] and is different from the situation in nuclear physics, where the exact energies fluctuate *around* the average ones.[16]

It is interesting to perform a liquid-drop-model–type expansion of the binding energies obtained in our calculations. This will be discussed in a forthcoming publication.[15] We only mention here that for neutral ($N=Z$) spherical Na clusters ($r_s=4$) our variational total energies are reproduced to within four digits for $N>8$ (*and within three digits even for* $N>2$) by

$$E(N)=a_v N+a_s N^{2/3}+a_c N^{1/3} . \tag{4}$$

Hereby $a_v=-0.1655$ Ry is the bulk energy, $a_s=0.0398$ Ry the surface energy, and $a_c=0.0113$ Ry the curvature energy coefficient. This value of the surface energy corresponds to a surface tension of $\sigma=155$ ergs cm^{-2}; the value found by Lang and Kohn[19] in microscopic Kohn-Sham calculations (using a slightly different correlation functional) for an infinite jellium surface with $r_s=4$ is $\sigma=160$ ergs cm^{-2}. This good agreement not only demonstrates the overall consistency of our results, but also the interesting fact that the Friedel oscillations, which are present in the density profiles of the Kohn-Sham results,[19] as well as in the microscopical densities of spherical clusters[3–5] (see Fig. 1), apparently do not contribute to the surface energy. In an independent recent study[20] for nucleons in typical potentials it has, in fact, been shown that Friedel oscillations hardly affect the surface energy, but contribute considerably (and negatively) to the curvature energy.

III. ELECTRONIC MULTIPOLE VIBRATIONS

A. RPA sum rules and inequalities

We shall now proceed to the discussion of collective vibrations of the valence electrons in spherical alkali-metal clusters. To this purpose, we shall employ the RPA sum-rule formalism.[13] We start from the RPA strength function $S_Q(E)$ corresponding to a given excitation operator $\hat{Q}$. The kth moments of $S_Q(E)$ are defined by

$$m_k(\hat{Q})=\int_0^\infty E^k S_Q(E)dE = \sum_{n\neq 0}(E_n)^k|\langle n|\hat{Q}|\tilde{0}\rangle|^2 . \tag{5}$$

Hereby E_n and $|n\rangle$ are the RPA energies and wave functions, respectively, of the excited states of the system, and $E_0=0, |\tilde{0}\rangle$ correspond to the RPA-correlated ground state. The operator $\hat{Q}$ is assumed here only to act upon the electron wave functions, i.e., we describe collective excitations of the electrons assuming the ionic background to be inert.

We shall be particularly interested in the moments m_3 and m_1 which can be expressed as the following ground-state expectation values, often called sum rules:

$$m_1(\hat{Q})=\tfrac{1}{2}\langle\tilde{0}|[\hat{Q},[\hat{H},\hat{Q}]]|\tilde{0}\rangle , \tag{6}$$

$$m_3(\hat{Q})=\tfrac{1}{2}\langle\tilde{0}|[[\hat{H},\hat{Q}],[\hat{H},[\hat{Q},\hat{H}]]]|\tilde{0}\rangle ; \tag{7}$$

hereby $\hat{H}$ is the total Hamiltonian of the system. The interest in these expressions lies in the fact that, according to a theorem by Thouless,[21] they can be evaluated replacing the correlated ground state $|\tilde{0}\rangle$ by the *uncorrelated* ground state $|0\rangle$ on the right-hand side of Eqs. (6) and (7), without introducing any error. That is, if one starts from a self-consistent microscopic Hartree-Fock calculation for a given Hamiltonian $\hat{H}$ and then performs a RPA calculation in terms of the HF particle-hole states to obtain the RPA spectrum $E_n, |n\rangle$, the full RPA moments m_3 and m_1 are obtained by taking the expectation values of the commutators in Eqs. (6) and (7) (*containing the same Hamiltonian*) in the HF ground state.

Note that the RPA moments m_k with other indices k can, in general, not be evaluated from the uncorrelated ground-state wave functions. It has, however, been shown[22] that the negative-energy-weighted sum rule m_{-1} is related to the static ground-state polarizability $\alpha_{\rm pol}(\hat{Q})$, which can be evaluated from a constrained HF variational procedure solving $\delta\langle\hat{H}-\lambda\hat{Q}\rangle=0$ with the Lagrange multiplier λ, by

$$m_{-1}(\hat{Q})=\tfrac{1}{2}\alpha_{\rm pol}(\hat{Q}) . \tag{8}$$

In the present case, we do not start from a HF solution but, ideally, from the solution of the Kohn-Sham equation derived from Eq. (1). Our semiclassical approach to the sum rules m_3 and m_1 consists[23] of evaluating exactly the commutators in Eqs. (6) and (7), and rewriting their expectation values as functionals of the density $\rho(r)$ using, where necessary, the semiclassical gradient expansions as will be shown below.

From the three moments (6)–(8), one gets the following inequalities[13] for the centroid $\bar{E}$ and the variance σ of the strength distribution $S_Q(E)$,

$$E_1\leq\bar{E}\leq E_3, \quad \sigma\leq\sigma_{\max}=\tfrac{1}{2}(E_3^2-E_1^2)^{1/2} , \tag{9}$$

in terms of the energies E_3, E_1 defined by

$$E_3=\left[\frac{m_3}{m_1}\right]^{1/2}, \quad E_1=\left[\frac{m_1}{m_{-1}}\right]^{1/2} . \tag{10}$$

It is thus possible to estimate the position and the width of a RPA mode, whose collective strength is concentrated in one peak, without performing the RPA calculation but simply by calculating the sum rules (6) and (7), and the static polarizability (8). [Note that if the peak

is infinitely narrow ($\sigma=0$), then $E_3 \equiv E_1$ is the energy of the collective state.]

For local operators $\hat{Q}=Q(\mathbf{r})$, the energies E_3 and E_1 have simple physical interpretations. As shown in Ref. 13, the moment m_3 then is the restoring force parameter ("spring constant") C and m_1 the inertial parameter B of a *diabatic* collective motion described in terms of the velocity (or rather displacement) field $\mathbf{u}(\mathbf{r})=-(\hbar^2/m)\nabla Q(\mathbf{r})$ (see also the Appendix). Thus, $E_3=\hbar\sqrt{C/B}=\hbar\omega$ is the energy of a harmonic vibration. This motion is diabatic in the sense that the electrons are oscillating around their equilibrium configurations without changing their nodal structure and without affecting their own mean field. One may therefore also call[24] E_3 the "sudden approximation" to the energy of the mode excited by the operator $\hat{Q}$. On the other hand, E_1 is the static or "adiabatic" approximation, since it involves the static polarizability via m_{-1}, see Eq. (8), thus describing a motion which is so slow that the mean field has time enough to follow self-consistently the oscillation of the electrons.

B. Surface plasmons

In order to describe collective electronic vibrations of multipolarity L, we shall first use the electric multipole operators in the long-wavelength limit (written in polar coordinates),

$$\hat{Q}=Q_L=r^L Y_{L,0}(\Theta,\phi) \quad (L\geq 1) . \tag{11}$$

These operators lead to divergence-free velocity fields, since $\Delta Q_L=0$, thus describing pure surface oscillations during which the electron density is translated ($L=1$) or deformed ($L>1$), but not compressed. Evaluation of the commutators in Eqs. (6) and (7) leads for spherical systems to[15,25]

$$\begin{aligned} m_1(Q_L)&=\frac{\hbar^2}{m}\frac{L}{2}\int r^{2L-2}\rho(r)d^3r , \\ m_3(Q_L)&=m_3^{\rm kin}+m_3^{\rm Coul}+m_3^{V_I} . \end{aligned} \tag{12}$$

The contribution of the kinetic energy to m_3 is

$$m_3^{\rm kin}=\left[\frac{\hbar^2}{m}\right]^2 L(L-1)\int r^{2L-4} \times\left[L\tau(r)+\frac{L-2}{2r^2}\lambda(r)\right]d^3r ; \tag{13}$$

the direct part of the electron-electron interaction gives

$$m_3^{\rm Coul}=-\left[\frac{\hbar^2}{m}\right]^2\frac{L^2(L-1)}{2L+1}(4\pi e)^2 \times\int_0^\infty r^{2L-3}\rho(r)dr\int_0^r r'^2\rho(r')dr' , \tag{14}$$

and the electron-ion interaction gives

$$m_3^{V_I}=\left[\frac{\hbar^2}{m}\right]^2\frac{L^2}{2(2L+1)} \times\int V_I(r)r^{2L-4}[r^2\rho''(r)+2rL\rho'(r)]d^3r , \tag{15}$$

where $\rho'(r),\rho''(r)$ are radial derivatives. Note that the exchange-correlation energy in the local-density approximation, like any part of the total energy which is only a *function* of $\rho(r)$, does not contribute to $m_3(Q_L)$.[13] In the kinetic-energy term (13), $\tau(r)$ is the kinetic-energy density and $\lambda(r)$ an angular momentum density, defined in terms of the Kohn-Sham single-particle wave functions $\varphi_i(\mathbf{r})$ by

$$\begin{aligned} \tau(\mathbf{r})&=\frac{\hbar^2}{2m}\sum_{i=1}^N|\nabla\varphi_i(\mathbf{r})|^2 , \\ \lambda(\mathbf{r})&=\frac{\hbar^2}{2m}\sum_{i=1}^N|\varphi_i(\mathbf{r})|^2 l_i(l_i+1) , \end{aligned} \tag{16}$$

where l_i is the angular momentum quantum number of the state i. Instead of the quantum-mechanical expressions (16) we use here the gradient-expanded ETF functional $\tau[\rho]$[7,8] and a corresponding functional $\lambda[\rho]$ which was recently derived,[23]

$$\lambda[\rho(\mathbf{r})]=\tfrac{2}{3}r^2\tau[\rho(\mathbf{r})]-\tfrac{1}{6}r^2\Delta\rho(\mathbf{r})+\tfrac{1}{2}\mathbf{r}\cdot\nabla\rho(\mathbf{r}) . \tag{17}$$

The above results simplify appreciably in the case of the dipole operator Q_1. Equation (12) with $L=1$ then becomes the familiar Thomas-Reiche-Kuhn sum rule

$$m_1(Q_1)=\frac{\hbar^2}{2m}N , \tag{18}$$

and the only contribution to m_3 comes from the electron-ion interaction, since all other terms in (1) are invariant with respect to a transition of the electrons. Writing the integrand in (15) for $L=1$ in terms of $\Delta\rho$, performing two partial integrations, and exploiting the Poisson equation for the ionic potential V_I, we find

$$m_3(Q_1)=\frac{1}{2}\left[\frac{\hbar^2}{m}\right]^2\frac{4\pi e^2}{3}\int\rho(r)\rho_I(r)d^3r . \tag{19}$$

Thus, the restoring force parameter (19) is, as could be expected, proportional to the overlap of the electron and the ion densities. Using the step function of the jellium model for the ionic density $\rho_I(r)$, we can write (19) as

$$m_3(Q_1)=\frac{1}{2}\left[\frac{\hbar^2}{m}\right]^2\frac{e^2}{r_s^3}(N-\Delta N) . \tag{20}$$

Hereby ΔN is the number of electrons outside the jellium, the so-called "spillout":

$$\Delta N=4\pi\int_{R_I}^\infty r^2\rho(r)dr . \tag{21}$$

With Eqs. (18) and (20) we find for the energy E_3 in the dipole case

$$\begin{aligned} E_3(Q_1)&=\left[\frac{\hbar^2}{m}\frac{e^2}{r_s^3}\left[1-\frac{\Delta N}{N}\right]\right]^{1/2} \\ &=\frac{1}{\sqrt{3}}\hbar\omega_{\rm pl}\left[1-\frac{\Delta N}{N}\right]^{1/2} , \end{aligned} \tag{22}$$

where $\hbar\omega_{\rm pl}$ is the plasma frequency. In the limit of a very large cluster, ΔN goes to zero and E_3 goes to the classical Mie result[26] for the dipole surface plasmon. (In Ref. 24 the same classical limit was recovered, although there the m_3 was evaluated differently and the leading contribution seemed to come from the electron-electron interaction.)

Note that our result (22) is quantum-mechanically exact, if $\rho(r)$ is evaluated from the Kohn-Sham wave functions; it holds for spherical clusters.

For the higher-multipolarity modes ($L>1$), we can in a similar way find the classical limit by assuming the electron density to be a step function with the value ρ_0^I. Neglecting the kinetic-energy contribution (13), which will be of order $N^{-2/3}$ relative to the leading Coulomb contributions, we get from (14) and (15) in this limit:

$$E_3(Q_L)\rightarrow\hbar\omega_L^{\rm Mie}=\left[\frac{L}{2L+1}\right]^{1/2}\hbar\omega_{\rm pl}\quad\text{for } N\rightarrow\infty\ , \tag{23}$$

which is the Mie result.[26]

We thus have found the novel result that the classical Mie frequency of the surface plasmon can be recovered from the RPA energy E_3, evaluating the sum rules in terms of the multipole operator (11), for any multipolarity L. For finite clusters there are surface and kinetic-energy corrections which will shift the energy away from this classical limit.

In Fig. 3 we show the energies $E_3(Q_L)=\hbar\omega_L$ for various multipolarities L, evaluated from our self-consistent semiclassical densities for Na clusters with atomic numbers N from 2 to 8000 (corresponding to radii R_I from $5a_0$ to $80a_0$). The dipole plasmon is red shifted due to the spillout factor $\Delta N/N$ in (22). For the higher L values, the kinetic-energy contribution (13) is nonzero and becomes more and more important for increasing L and decreasing size of the cluster. As a result, the $\hbar\omega_L$ with $L>1$ are *larger* than the Mie energies for small clusters; only in the large-N limit, where the kinetic-energy contribution becomes negligible, do they approach the Mie limit from below.

Our results for E_3 in the dipole case agree well with the values quoted by Bertsch and Ekardt[24]—there called ω(sudden)—within 2 parts per thousand for the clusters with $N=20$ and 90; in the case with $N=192$ our value is $\sim 2\%$ larger.

C. Coupling between surface and volume plasmons

We have included in Fig. 3 also a volume plasmon with multipolarity $L=0$ which is analogous to the "breathing-mode" vibration (giant monopole resonance) of nuclei. We chose for this mode the operator $Q_0=r^2$, which leads to a good approximation of the breathing-mode energies in heavy nuclei.[13,23] With this operator, all terms in the energy (1) contribute to the restoring force parameter m_3; the energy E_3 can be written as

$$E_3(Q_0)=\left[\frac{\hbar^2 K_N N^{2/3}}{m\langle r^2\rangle}\right]^{1/2}\ , \tag{24}$$

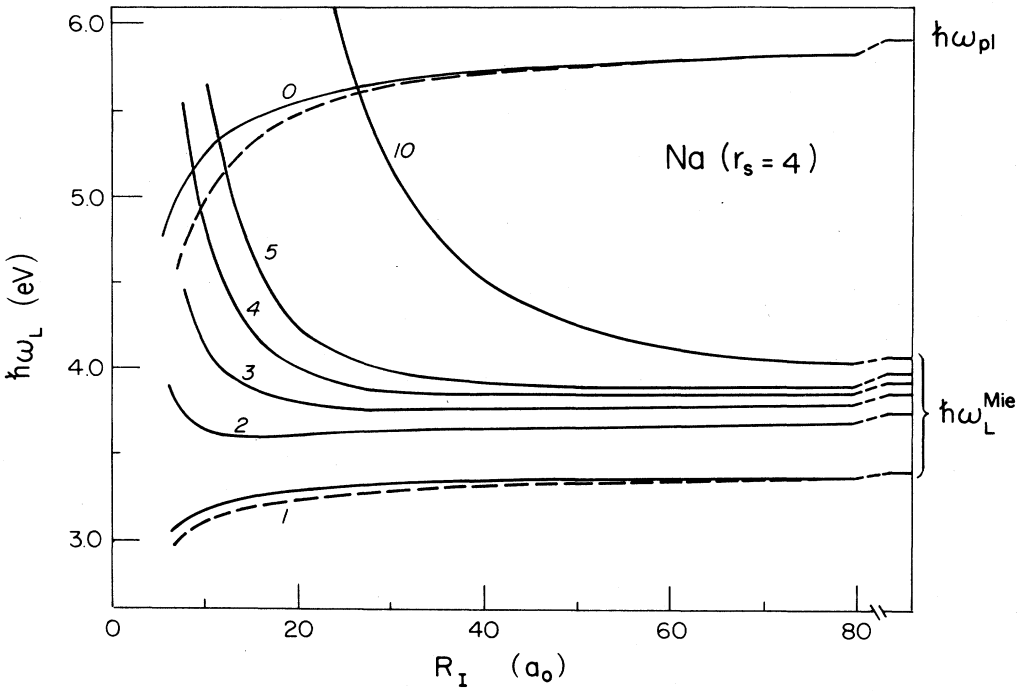

FIG. 3. Plasmon frequencies $\hbar\omega_L=E_3(Q_L)$ for finite Na clusters vs radius R_I. The solid curves labeled 1, . . . , 5 and 10 are the surface plasmons of corresponding multipolarity L; the solid line labeled 0 is the volume plasmon. The plasma frequency $\hbar\omega_{\rm pl}$ and the Mie surface-plasmon frequencies $\hbar\omega_L^{\rm Mie}$ are shown on the right-hand margin of the figure to be reached asymptotically for $N\rightarrow\infty$. The dashed lines show the centroids of the eigenvalue spectrum for $L=0$ and 1, respectively, as calculated below (see text for details).

where K_N is the incompressibility of the N cluster and $\langle r^2 \rangle$ is its mean-squared radius. We leave the detailed formula for K_N and its discussion for a future publication[15] and just mention here that K_N can be expanded as

$$K_N = \frac{9}{5}\frac{e^2}{r_s} + O(N^{-1/3}) + \cdots \ . \tag{25}$$

It might be of interest to note that the leading term in (25) corresponds to bulk compression moduli for alkali metals which are within less than 15% of the experimental ones. In the classical limit we recover from $E_3(Q_0)$ in (24) the plasmon frequency

$$E_3(Q_0) \to \hbar\omega_{\rm pl} \quad \text{for } N \to \infty \ , \tag{26}$$

as can also be seen from the results in Fig. 3.

In finite clusters we have to expect a coupling of surface and volume plasmons for all multipolarities, as pointed out by Ekardt[6] in the dipole case. In order to study such a coupling in our present approach, we introduce a set of trial operators Q_L^p for each multipolarity:

$$Q_L^p = r^p Y_{L,0}(\Theta,\phi) \tag{27}$$

with p being a positive real number. For $p \neq L$, $\Delta Q_L^p \neq 0$ and this operator will describe modes which involve local compression of the electrons, such as is the case for the r^2 operator (Q_0) discussed above. We therefore study the coupling of modes obtained with (27) using different values of p. We use hereby a multidimensional extension of the sum-rule approach which was recently developed for describing giant resonances in nuclei.[23]

Noting, as discussed above, that E_3 is the one-phonon energy of a harmonic oscillator with spring constant $C = m_3$ and mass $B = m_1$, it is a natural extension of Eqs. (6) and (7) to introduce the following matrices:

$$B_{pp'} = \tfrac{1}{2}\langle 0|[Q_L^p,[\hat{H},Q_L^{p'}]]|0\rangle \ , \tag{28}$$

$$C_{pp'} = \tfrac{1}{2}\langle 0|[[[\hat{H},Q_L^p],[\hat{H},[Q_L^{p'},\hat{H}]]]|0\rangle \ . \tag{29}$$

They are symmetric as long as $|0\rangle$ is an eigenstate of $\hat{H}$. [Note that the right-hand sides of Eqs. (28) and (29) can again be identified, by an extension[13] of the proof given by Thouless, with the corresponding sum rules of a mixed RPA strength function involving the transition probabilities $\langle \tilde{0}|Q_L^p|n\rangle\langle n|Q_L^{p'}|\tilde{0}\rangle$.]

The stiffness tensor $C_{pp'}$ and the mass tensor $B_{pp'}$ define a system of coupled harmonic oscillators. Choosing now a series of M operators with different values p_i ($i = 1,2,\ldots,M$) for a given L, we can solve the secular equations

$$\sum_{j=1}^{M} (C_{p_i p_j} - \omega_n^2 B_{p_i p_j}) x_j^n = 0 \quad (i,n = 1,\ldots,M) \tag{30}$$

in order to find M eigenmodes of multipolarity L with frequencies ω_n and eigenvectors x_j^n. These eigenmodes have velocity fields $\mathbf{u}_n$ fulfilling the orthogonality relation

$$m\int \mathbf{u}_n \cdot \mathbf{u}_m \rho(\mathbf{r}) d^3r = \tilde{B}_n \delta_{nm} \ , \tag{31}$$

where $\tilde{B}_n$ is the mass of the nth normal mode. For a given excitation operator $\hat{Q}$, we then calculate the sum rules m_k semiclassically by

$$m_k(\hat{Q}) = \sum_{n=1}^{M} (\hbar\omega_n)^k |\langle n|\hat{Q}|0\rangle|^2_{\rm sc} \ , \tag{32}$$

where the semiclassical transition probabilities are

$$|\langle n|\hat{Q}|0\rangle|^2_{\rm sc} = \frac{\hbar}{2\omega_n \tilde{B}_n}\left|\int \hat{Q}\delta\rho_n d^3r\right|^2 \ , \tag{33}$$

and $\delta\rho_n$ is the transition density from the ground state to the one-phonon state with energy $\hbar\omega_n$:

$$\delta\rho_n = -\nabla\cdot(\rho\mathbf{u}_n) \ . \tag{34}$$

By construction,[23] Eq. (32) gives the correct RPA sum rules $m_1(Q)$ and $m_3(Q)$ for local operators Q whose gradients lie in the space spanned by the $\mathbf{u}_n$, i.e., the eigenmode spectrum of Eq. (30) exhausts these two sum rules. Although this cannot be proven for the other moments, we may take Eq. (32) as a semiclassical approximation to the corresponding RPA moments. Evaluating in this way the moments m_{-1}, m_0, and m_2, we can obtain our estimates for the static polarizabilities by Eq. (8) and the centroids $\bar{E}$ and variances σ of the strength function by

$$\bar{E} = \frac{m_1}{m_0}, \quad \sigma^2 = \frac{m_2}{m_0} - \left[\frac{m_1}{m_0}\right]^2 \ . \tag{35}$$

The evaluation of Eqs. (28) and (29) with our trial operators (27) is rather cumbersome for $p,p' \neq L$, particularly for the kinetic-energy contribution to the stiffness tensor (29). We have evaluated the latter contribution in the local-density approximation, i.e., using the Thomas-Fermi functional $\tau[\rho]$ for the kinetic energy, in the cases with $p,p' \neq L$. (For not overly small clusters, the corresponding terms will not contribute appreciably.) The explicit results in terms of integrals over the density $\rho(r)$ are given in the Appendix. We shall first discuss the classical limit, for which the results are analytical, and then give numerical results for the finite clusters.

In the classical limit of a very large cluster, the diffuseness of the electron density can be ignored, so that we can take ρ to be a step function: $\rho(r) = \rho_0^I \Theta(R_I - r)$. Furthermore, the kinetic and exchange-correlation energies vanish as $N^{-2/3}$ with respect to the leading Coulomb contributions. We then find from Eqs. (A4), (A10), and (A11) the following analytical results:

$$B_{pp'} = \frac{\hbar^2}{2m}\frac{3N}{2L+1}\frac{R_I^{p+p'-2}}{p+p'+1}[pp' + L(L+1)] \ , \tag{36}$$

$$C_{pp'} = \frac{1}{2}\left[\frac{\hbar^2}{m}\right]^2 \frac{3e^2}{r_s^3}\frac{3N}{2L+1}\frac{R_I^{p+p'-2}}{p+p'+1} \times \left[pp' + \frac{L(L+1)}{2L+1}(2L-p-p')\right] \ , \tag{37}$$

valid for all $L \geq 0$ and $p+p' > -1$. Solving the secular equations (30) with the matrices (36) and (37) for a given set of M different numbers p_i leads to the following interesting results.

(1) *Case* $L = 0$. Independently of the values of p_i (trivially, they must all be positive), there is only one (M-fold)-

degenerate eigenvalue $\omega=\omega_{\rm pl}$. This is seen directly from the above expressions with $L=0$ in which case $C_{pp'}/B_{pp'}=\omega_{\rm pl}^2$ for all p and p'. There exists thus for classical metal spheres only one monopole mode with the same frequency as the bulk plasmon.

(2) *Case* $L>0$. There are always $M-1$ degenerate eigenvalues $\omega=\omega_{\rm pl}$, independently of the p_i, and one nondegenerate eigenvalue $\omega_L\neq\omega_{\rm pl}$. If one of the p_i equals L, then ω_L is the classical Mie frequency of the surface plasmon: $\omega_L=\omega_L^{\rm Mie}$. If all the p_i are different from L, then $\omega_L\simeq\omega_L^{\rm Mie}$, whereby $\omega_L\to\omega_L^{\rm Mie}$ for $M\to\infty$. (We have no mathematical proof for this general result but checked it numerically for many instances.) Thus, in classical metal spheres there exist for each multipolarity L a surface plasmon with the Mie frequency and a volume plasmon with the bulk-plasmon frequency. It should be noted that in this classical limit the surface plasmon takes up all of the strength of the multipole operator Q_L, and the volume plasmons are decoupled.

The fact that all volume plasmons are degenerate in the classical limit means that the energies E_3 of these solutions do not depend on the radial form of the operator Q. This in itself is not surprising since this limit is *defined* as the one where the electron density is constant over the whole volume of the cluster.

Our result for $L>0$ is a generalization of the result of Jensen,[27] who in 1937 investigated the dipole oscillations of small metal spheres by solving the hydrodynamical equations of motion with the boundary condition of a step function for the electron density. He found small derivations of the above frequencies of the order R_I^{-1}, which also in our present treatment come about naturally as soon as one allows for $\rho(0)\neq\rho_0^I$, or if one takes kinetic energy, exchange-correlation effects, or a finite diffusivity of the electron density into account. These effects thus lift the degeneracy of the volume plasmons and give them a finite multipole strength in real finite clusters.

In our numerical calculations we evaluated Eqs. (28) and (29) from the variational ground-stated densities $\rho(r)$ of finite clusters. The choice of the number M of coupled modes, as well of the values p_i used to obtain the eigenmode spectrum, was made by trial and error. We found that typically the results for $\bar{E}$, σ, and the polarizabilities $\alpha_{\rm pol}$ converged within a few percent (the $\alpha_{\rm pol}$ being the most sensitive ones) for $8\lesssim M\lesssim 12$ and $1\lesssim p_i\lesssim 12$, the upper limits being given by purely numerical stability reasons. The resulting centroid energies $\bar{E}$ for the monopole and the dipole cases are shown in Fig. 3 above by the dashed lines. The difference to the solid line indicates in the dipole case the coupling between the surface and the volume modes; it disappears in the limit $N\to\infty$, as mentioned above. In the monopole case, the difference comes from the admixture of modes corresponding to values of p_i different from 2 (which was used for the solid line in Fig. 3).

For the remaining discussion of our results, we shall restrict ourselves to dipole oscillations, as they have recently been observed experimentally by photoabsorption on small Na clusters.[28] As already mentioned, our results for the E_3 energies obtained with the dipole operator agree very well with those of the microscopic Kohn-Sham calculations.[6,24]

In Fig. 4 we show by the solid line our results for the static dipole polarizabilities $\alpha_{\rm pol}$ of spherical Na clusters obtained from the moments $m_{-1}(Q_1)$ with Eq. (8). They are seen to reproduce fairly well—apart from some weak shell effects—the microscopic results obtained in the same jellium model with LDA exchange and correlations,[4-6,29] shown by the squares. They share the common defect of all LDA calculations to underestimate the measured polarizabilities[30] by $\sim$20–25 %. This defect is presumably due to the LDA treatment of the Coulomb exchange. As a consequence of this approximation, there is too much screening of the external potential V_I by the electrons, which lets the total (Kohn-Sham) potentials fall off too quickly in the surface of the clusters. This, in turn, leads to a too steep tail of the electron densities and an underestimation of the spillout factor $\Delta N/N$ defined by Eq. (21). As has been shown,[4,11] the static polarizability is closely related to this spillout, so that an increased ΔN will lead to an increased $\alpha_{\rm pol}$. Indeed, in a recent investigation[29] a self-interaction correction,[31] which cures some of the deficiencies of the LDA treatment of the Coulomb exchange in a somewhat *ad hoc* way, was used within the Kohn-Sham approach and shown to lead to a considerable improvement of the static polarizabilities towards the experimental results.

As stated in Sec. III A, the static polarizability $\alpha_{\rm pol}$ can, in principle, be calculated from a variational calculation with an external constraint, as it has been done both microscopically[4,5,29] and semiclassically.[11] Our results in Fig. 4 are obtained differently, namely over the sum rule equation (8) using our "semiclassical RPA" spectrum. The fact that they agree exactly with those of Snider and Sorbello,[11] as well as with the microscopic ones to the extent shown in Fig. 4, gives some confidence in the moments m_k of this spectrum.

We shall finally address ourselves to the collective dipole vibration recently observed experimentally in small

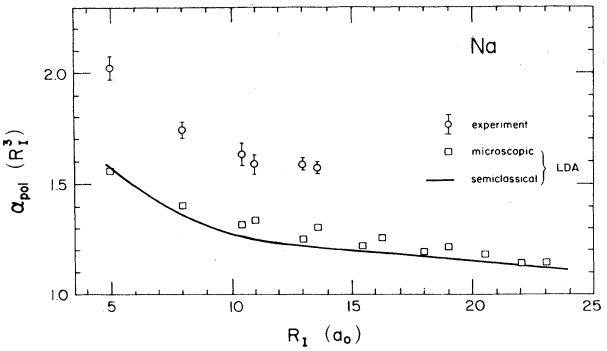

FIG. 4. Static dipole polarizabilities of spherical Na clusters, in units of the classical value R_I^3, vs radius R_I. Solid line shows present results obtained over the m_{-1} sum rule (8). Squares are microscopic results (Refs. 4–6 and 29). Experimental values from Knight *et al.* (Ref. 30).

sodium clusters by photoabsorption.[28] We only compare here our results for the spherical Na_8 cluster. The peak of the resonance curve seen[28,32] in Na_8 lies at about 2.5 eV. Our result for the centroid $\bar{E}$ obtained for the dipole (see Fig. 3) is 3.0 eV, very close to the peak value of Ekardt.[6] This shift has the same origin as the deficiency of the static polarizabilities discussed above and will, hopefully, be removed in a better treatment of the Coulomb exchange.

It is also interesting to compare the width extracted from the sum rules above. Unfortunately, the dipole m_1 sum rule is only exhausted to $\sim 55-65\,\%$ by the experimental cross section,[32] depending somewhat on the assumed form of the resonance curve. Evaluating numerically the various moments of the experimental cross section in the measured frequency region, we find a variance $\sigma_{\rm expt}=0.18$ eV. (Note that this is the variance and not the width [full width at half maximum (FWHM)].) The values found from our semiclassical results above via Eqs. (9) and (35) are $\sigma_{\rm max}=0.50$ eV and $\sigma=0.47$ eV. This RPA variance reflects the fragmentation of the dipole strength due to the coupling of surface and volume vibrations. Note, however, that it is the variance of the *total* dipole strength distribution, taking also into account energy regions in which no strength has been seen experimentally (as is reflected in the missing strength mentioned above), and is thus appreciably larger. Also, our treatment does not take into account any coupling of the electronic motion to that of the ions. Indeed, it was recently pointed out[33] that shape vibrations of the ionic background lead to widths comparable to the measured one, even if the intrinsic RPA width of the electronic dipole resonance is assumed to be an order of magnitude smaller.

A simple qualitative estimate for the asymptotic size dependence of the variance of the dipole resonance in large clusters, based on the upper estimate $\sigma_{\rm max}$ defined in Eq. (9), is obtained as follows. The static dipole polarizabilities are often parametrized as

$$\alpha_{\rm pol}=(R_I+\delta)^3 \ . \tag{38}$$

It has been shown[4,11] that for large clusters δ is approaching a constant asymptotic value[19] δ_p which for sodium clusters ($r_s=4a_0$) equals $1.3a_0$. Using Eqs. (8), (10), and (18) we get

$$\lim_{N\to\infty} E_1(Q_1)=\hbar\omega_{L=1}^{\rm Mie}\left[1-\frac{3\delta_p}{R_I}\right]^{1/2} . \tag{39}$$

On the other hand, the spillout factor defined by Eq. (21) goes as

$$\lim_{N\to\infty}\frac{\Delta N}{N}=\frac{3\zeta}{R_I} \ , \tag{40}$$

where ζ asymptotically is also a constant. For sodium clusters we find from our semiclassical results the value $\zeta=0.47a_0$. With Eq. (22) we now have

$$\lim_{N\to\infty} E_3(Q_1)=\hbar\omega_{L=1}^{\rm Mie}\left[1-\frac{3\zeta}{R_I}\right]^{1/2} . \tag{41}$$

Combining Eqs. (40) and (41) with (9), we thus obtain

$$\lim_{N\to\infty}\sigma_{\rm max}^{\rm dipole}=\tfrac{1}{2}\hbar\omega_{\rm pl}\left[\frac{\delta_p-\zeta}{R_I}\right]^{1/2} \simeq 0.23\hbar\omega_{\rm pl}N^{-1/6} \ \text{ for Na} \ . \tag{42}$$

This result reflects again the vanishing coupling of surface and volume vibrations for large clusters.

IV. SUMMARY AND CONCLUSIONS

We have presented a semiclassical density-variational method for the calculation of average properties of metal clusters within the jellium model. We have obtained a very detailed reproduction of the averaged results of the corresponding microscopic Kohn-Sham calculations for the static properties of spherical alkali clusters. In particular, our method allows one to calculate very efficiently the average self-consistent potentials which later may be used in microscopic calculations as a starting point. Due to the simplicity of our method which does not involve any wave functions, there are no limitations to the sizes of the clusters.

In a second step we have presented a "semiclassical RPA" method, making use of sum-rule relations, to calculate a spectrum of eigenmodes explicitly taking into account the coupling between surface and volume plasmons in finite clusters. We have shown how the classical Mie frequencies of the surface plasmons emerge from the RPA sum rules in the classical limit of very large metal spheres. Similarly, the monopole ($L=0$) vibration, which is analogous to the breathing mode of nuclei, was shown in the classical limit to have the plasma frequency $\hbar\omega_{\rm pl}$. From the moments of our eigenmode spectra we could estimate the mean positions (centroids) and variances of collective electronic vibrations, in the dipole case in good agreement with the results of Ekardt's much more time-consuming TDLDA calculations.[6,24]

It is thus hoped that the method presented here may be helpful to investigate in an economical way the average properties of metal clusters, and also those containing many thousands of atoms where microscopic calculations become impossible, as well as to provide an almost self-consistent starting point for more detailed microscopic investigations wherever those are feasible. Based on the experience made with similar methods in nuclear physics,[9] we expect to be able to incorporate the shell effects in binding and deformation energies and work functions accurately and economically either by the Strutinsky method[16] or by adding one or a few Kohn-Sham iterations, both based on the semiclassically obtained self-consistent average energies and potentials. Investigations along these lines are in progress.

Note added in proof: We have meanwhile calculated the kinetic-energy contribution to the stiffness tensor (29) *quantum mechanically* also for $p,p'\neq L$ in the dipole case ($L=1$), obtaining an expression of similar structure as in Eq. (13), but with complicated coefficients depending on p and p'. Using at the same time improved computer routines for the numerical solution of the secular equations (30), we find results for both $\bar{E}$, σ, *and* $\alpha_{\rm pol}$ that are stable

within less than 1 part per thousand for $4 \lesssim M \lesssim 12$ and $1 \leq p_i \lesssim 15$. (A four-digit accuracy is typically obtained for all cluster sizes coupling the $M=4$ modes with $p_i=1$, 4, 7, and 10.) The resulting $\alpha_{\rm pol}$ is *lower* than the one shown in Fig. 4 (solid line) by $\sim 5\%$ for $N=2$, by $\sim 3\%$ for $N=8$, and by less than 1% for $N \geq 20$ ($R_I \gtrsim 11 a_0$). The method of solving the secular equations (30), evaluating Eqs. (28) and (29) quantum mechanically with the *most general* set of (eventually nonlocal) operators $\hat{Q}^p_L$, is completely equivalent to a fully microscopic RPA calculation and thus leads to the exact RPA spectrum of multiplarity L.

ACKNOWLEDGMENTS

I am deeply indebted to W. Knight and S. Bjørnholm for stimulating my interest in metal clusters, for many helpful discussions, and their continuing interest in this research. Clarifying discussions with B. Mottelson, H. Nishioka, and P. G. Reinhard are gratefully acknowledged. I want to thank the Niels Bohr Institute for its hospitality and its computer staff for excellent working conditions during a research visit, and the Danish Research Council for financial support.

APPENDIX: EVALUATION OF EQS. (28) AND (29)

The evaluation of the commutators in Eqs. (28) and (29) is greatly simplified due to the scaling properties[13] of the commutator $[\hat{H},\hat{Q}]$ of a local operator Q which commutes with the potential-energy parts in $\hat{H}$, as is the case for the operators Q^p_L in Eq. (27). Let us define the "scaling operator" $\hat{S}^p_L$ by

$$\hat{S}^p_L=[\hat{H},Q^p_L]=[\hat{T},Q^p_L]=\tfrac{1}{2}(\nabla\cdot\mathbf{u}^p_L)+\mathbf{u}^p_L\cdot\nabla \ , \tag{A1}$$

where $\hat{T}$ is the kinetic-energy operator and $\mathbf{u}^p_L$ is the displacement field corresponding to the operator Q^p_L:

$$\mathbf{u}^p_L(\mathbf{r})=-\frac{\hbar^2}{m}\nabla Q^p_L(\mathbf{r}) \ . \tag{A2}$$

The mass tensor $B_{pp'}$ defined in Eq. (28) is easily shown by partial integration to be equal to

$$B_{pp'}=\frac{m}{2\hbar^2}\int \mathbf{u}^p_L(\mathbf{r})\cdot\mathbf{u}^{p'}_L(\mathbf{r})\rho(\mathbf{r})d^3r \ . \tag{A3}$$

For spherical densities $\rho(r)$ we find after performing the angular integrations

$$B_{pp'}=\frac{\hbar^2}{2m}\frac{pp'+L(L+1)}{2L+1}(4\pi)\int_0^\infty r^{p+p'}\rho(r)dr \ . \tag{A4}$$

The stiffness tensor $C_{pp'}$ defined in Eq. (29) is more cumbersome to evaluate. With the definition of the scaling operators in Eq. (A1) we can rewrite it as

$$C_{pp'}=\tfrac{1}{2}\langle 0|[\hat{S}^p_L,[\hat{S}^{p'}_L,\hat{H}]]|0\rangle$$
$$=\frac{1}{2}\left[\frac{d^2}{d\alpha\, d\alpha'}\langle 0|e^{\alpha\hat{S}^p_L}\hat{H}e^{-\alpha'\hat{S}^{p'}_L}|0\rangle\right]_{\alpha=\alpha'=0} \ . \tag{A5}$$

After some lengthy algebra, the results can be given in the following way. We write

$$C_{pp'}=C^{\rm kin}_{pp'}+C^{\rm xc}_{pp'}+C^{\rm Coul}_{pp'}+C^{V_I}_{pp'} \ . \tag{A6}$$

Note that even if $\hat{S}^p_L$ and $\hat{S}^{p'}_L$ do not commute, $C_{pp'}$ in Eq. (A5) is symmetric as long as $|0\rangle$ is an eigenstate of $\hat{H}$. This is, however, not true for each of the single contributions in (A6). Furthermore, we are only using an approximate ground-state density $\rho(r)$. It is therefore reasonable to symmetrize the single terms in (A6) separately.

The kinetic-energy (for $p,p' \neq L$) and the exchange-correlation contributions have been evaluated in the local-density approximation, which for the kinetic energy means using the Thomas-Fermi functional

$$\tau[\rho]=\frac{\hbar^2}{2m}\tfrac{3}{5}(3\pi^2\rho)^{2/3}\rho \ . \tag{A7}$$

These two contributions then are obtained using the following formula which holds for any part of the energy that is just a spatial integral over a *function* f of the density $\rho(r)$. Let E_f be given by

$$E_f=E_f[\rho]=\int f(\rho(r))d^3r \ . \tag{A8}$$

Then the symmetrized contribution of E_f to (A5) is found to be

$$C^f_{pp'}=\left[\frac{\hbar^2}{2m}\right]^2\frac{4\pi}{2L+1}\int_0^\infty r^{p+p'-2}\left[(p+p'-1)\{p[p'(p'+1)-L(L+1)]+p'[p(p+1)-L(L+1)]\}\left[f(\rho)-\rho\frac{df(\rho)}{d\rho}\right]\right.$$
$$\left.+2[p(p+1)-L(L+1)][p'(p'+1)-L(L+1)]\rho^2\frac{d^2f(\rho)}{d\rho^2}\right]dr \ , \tag{A9}$$

and holds for $L \geq 0$ and $p+p' \geq 2$. The symmetrized Hartree-Coulomb contribution to $C_{pp'}$ is

$$C^{\rm Coul}_{pp'}=\left[\frac{\hbar^2}{m}\right]^2\frac{(4\pi e)^2}{2(2L+1)}\int_0^\infty\rho(r)\left[\tfrac{1}{2}[(p+p')L(L+1)+pp'(p+p'-6)]r^{p+p'-3}\int_0^r r'^2\rho(r')dr'\right.$$
$$+\frac{L(L+1)}{2L+1}\left[(L-p')(p+L+1)r^{p'-L-1}\int_0^r r'^{L+p}\rho(r')dr'\right.$$
$$\left.\left.+(L-p)(p'+L+1)r^{p-L-1}\int_0^r r'^{L+p'}\rho(r')dr'\right]\right]dr \ , \tag{A10}$$

valid for $L \geq 0$ and $p+p' \geq 0$. The contribution from the external jellium potential V_I finally is

$$C_{pp'}^{V_I}=\left[\frac{\hbar^2}{2m}\right]^2\frac{4\pi}{(2L+1)}\int_0^\infty V_I(r)r^{p+p'-2}\left\{(p+p'-1)[(p+p'+2)pp'-(p+p')L(L+1)]\rho(r)\right.$$
$$\left.+[(3p+3p'-2)pp'-(p+p')L(L+1)]r\frac{d\rho(r)}{dr}+2r^2pp'\Delta\rho(r)\right\}dr \qquad \text{(A11)}$$

for $L\geq 0$ and $p+p'\geq 2$.

In the case $p=p'=L$ we recover from the above equations the results given in Eqs. (12), (14), and (15). [But *not* the kinetic contribution in Eq. (13), which was calculated quantum mechanically.]

---

*Permanent address: Institute of Theoretical Physics, University of Regensburg, D-8400 Regensburg, Federal Republic of Germany.

[1]W. D. Knight, W. A. de Heer, and K. Clemenger, Solid State Commun. **53**, 445 (1985).
[2]J. L. Martins, R. Car, and J. Buttet, Surf. Sci. **106**, 261 (1981).
[3]W. Ekardt, Phys. Rev. B **29**, 1558 (1984).
[4]D. E. Beck, Phys. Rev. B **30**, 6935 (1984).
[5]M. Manninen, R. M. Nieminen, and M. J. Puska, Phys. Rev. B **33**, 4289 (1986).
[6]W. Ekardt, Phys. Rev. B **31**, 6360 (1985); **32**, 1961 (1985).
[7]C. H. Hodges, Can. J. Phys. **51**, 1428 (1973).
[8]C. Guet and M. Brack, Z. Phys. A **297**, 247 (1980).
[9]M. Brack, C. Guet, and H.-B. Håkansson, Phys. Rep. **123**, 275 (1985), and the literature quoted therein.
[10]M. Cini, J. Catal. **37**, 187 (1975).
[11]D. R. Snider and R. S. Sorbello, Phys. Rev. B **28**, 5702 (1983); Solid State Commun. **47**, 845 (1983).
[12]V. Kresin, Phys. Rev. B **38**, 3741 (1988).
[13]O. Bohigas, A. M. Lane, and J. Martorell, Phys. Rep. **51**, 267 (1979), and the literature quoted therein.
[14]O. Gunnarsson and B. I. Lundqvist, Phys. Rev. B **13**, 4274 (1976).
[15]M. Brack (unpublished).
[16]V. M. Strutinsky, Nucl. Phys. **A122**, 1 (1968); see also M. Brack and P. Quentin, *ibid.* **A361**, 35 (1981).
[17]W. Ekardt and Z. Penzar, Phys. Rev. B **38**, 4273 (1988).
[18]R. K. Bhaduri, M. Brack, H. Gräf, and P. Schuck, J. Phys. (Paris) Lett. **41**, L347 (1980).
[19]N. D. Lang and W. Kohn, Phys. Rev. B **1**, 4555 (1970).
[20]S. Vydrug-Vlasenko and M. Brack (unpublished).
[21]D. J. Thouless, Nucl. Phys. **22**, 78 (1961).
[22]E. R. Marshalek and J. da Providência, Phys. Rev. C **7**, 228 (1973).
[23]P. Gleissl, M. Brack, J. Meyer, and P. Quentin (unpublished).
[24]G. Bertsch and W. Ekardt, Phys. Rev. B **32**, 7659 (1985).
[25]See also M. Casas and J. Martorell, An. Fis. (Spain) **81**, 150 (1985), for the kinetic and Hartree-Coulomb contributions to m_3.
[26]G. Mie, Ann. Phys. (Leipzig) **25**, 377 (1908).
[27]H. Jensen, Z. Phys. **106**, 620 (1937).
[28]W. A. de Heer *et al.*, Phys. Rev. Lett. **59**, 1805 (1987).
[29]P. Stampfli and K. H. Bennemann, in *Physics and Chemistry of Small Clusters*, Vol. 158 of *NATO Advanced Study Institute Series B: Physics*, edited by P. Jena, B. K. Rao, and S. N. Khanna (Plenum, New York, 1987) p. 473.
[30]W. Knight *et al.*, Phys. Rev. B **31**, 2539 (1985).
[31]J. P. Perdew and A. Zunger, Phys. Rev. B **23**, 5048 (1981).
[32]K. Selby *et al.*, Z. Phys. D (to be published); W. Knight (private communication).
[33]G. Bertsch and D. Tománek (unpublished).